

Department of Electrical and Computer Systems Engineering

Technical Report MECSE-23-2004

MODELLING OF POLARISATION MODE DISPERSION EFFECT
SYSTEM USING FINITE IMPULSE RESPONSE DISCRETE FILTER
TECHNIQUE

LN Binh and A. Selliah

MONASH
UNIVERSITY

MODELLING OF POLARISATION MODE DISPERSION EFFECTS IN A DWDM SYSTEM USING FINITE IMPULSE RESPONSE DISCRETE FILTER TECHNIQUE

Le Nguyen Binh and Ashok Selliah

Department of Electrical and Computer Systems Engineering, Monash University, Wellington Road, Clayton, Victoria 3168 Australia

Abstract

Modelling of optical fibre systems has been normally performed without much considerations of the bi-modal nature of the weakly guided fundamental linearly polarised mode propagation and hence minimum accommodation of polarisation-related effects such as the polarisation-mode dispersion (PMD) of first and higher orders that further reduce the performance of optical communication systems, especially at bit rates in the region of 40 Gb/s. A vector field propagation taking into account both polarisation modes of transmission would thus be necessary and a modelling method that would optimise the computing resources are desired.

In this paper, a time-domain simulation is developed employing transmission matrix method for the two-mode propagation and the representation of the chromatic dispersion and PMD using discrete filter technique are proposed. The effects of chromatic dispersion and PMD could be integrated into the nonlinear Schrodinger equation by representing the pulse broadening as linear infinite impulse responses. Furthermore the PMD effects are generated using the widely known statistical model and the chromatic dispersion is also modelled as a discrete filter in the z-transform domain in lieu of the normal FFT-based filters. This enhances the computational resources under the time domain propagation approach. The performance of the simulation package was measured by propagating a 10Gbps and 40 Gb/s DWDM systems.

TABLE OF CONTENTS

1. Introduction	3
2. The Propagation equation	5
2.1 Generic dispersion in single mode fibres	5
2.2 Polarization Mode Dispersion	7
2.3 Field Propagation Equation	9
3. Modelling Platform	9
3.1 Time domain approach	10
3.2 IIR filter for chromatic dispersion	13
4. Design of IIR filters	13
4.1 Inclusion of PMD phenomena	19
4.2 Algorithm for the split step model	20
4.3 Representation of the optical signal	24
4.4 Optical source modelling	24
4.5 Sampling of the input waveform:	25
5. Case study	26
5.1 Simulation of 10Gpbs System	27
5.2 Simulation of A 40Gb/s communication system	32
6. Conclusions	34
7. References	35

Figure 1 Schematic illustration of symmetrised split step model used for numerical simulations.....	10
Figure 2 Cascade of optical transfer functions representing the vector field propagation.	11
Figure 3 The plot of delay term $\frac{u(1-u^2)}{(1+u^2)^2}$ as a function of u.....	15
Figure 4 Cascade for obtaining greater group delay PMD effects.....	15
Figure 5 Comparison of the ideal group delay verus the IIR filter produced group delay	17
Figure 6 Signal power channel output at the start of transmission	28
Figure 7 The 10 Gbps transmitted bits after 10 Km of propagation.....	29
Figure 8 Resulting output spectrum of multiplexed channels after 10Km of the 10Gb/s channel.....	30
Figure 9 The power output channels 1 to 4 after 30 km of propagation.....	31
Figure 10 Output power of channel 1 at the start of simulation for a 40G/s system	33
Figure 11 Output signal power of channel 1 after 30 kms of propagation	33
Figure 12: Effects of PMD on channel 1 and channel 2 after transmission	34
Table 1: The filter parameters for measuring filter performance	16
Table 2 Corning SMF-28™ fibre specifications.....	27
Table 3 Simulation set up for propagation of 10Gb/s.....	27
Table 4 TeraLight™ 6910 fibre specifications	32

1. Introduction

The deployment of optical fibre communications systems has been growing rapidly over the past few decades. The low loss and wide bandwidth of the new generation optical fibres makes it ideal for long-haul and high bit-rate transmission systems. The use of optical amplification technique for increasing the repeater spacing and wavelength division multiplexing (WDM) for increasing the line rate have allowed for the deployment of 10 Gb/s x 160 wavelength-multiplexed optical communication systems throughout the world [1], [2]. The transmitted optical pulse sequences are subjected to chromatic dispersion, loss, the polarisation mode dispersion (PMD) and nonlinearity depending on the fibre guiding properties. These effects place a limit on the transmission rate of long-haul communication systems. If the optical pulses degrade significantly, it would be impossible to recover the original signal input at the transmitter end. As the transmission line rate is increased up to and beyond 40 Gb/s, the dispersion of the transmission medium in a single mode optical fibre, becomes very critical for error-free transmission. The *dispersion* effects of a single mode optical fibre include the normal chromatic dispersion consisting of the fibre silica material dispersion due to the variation of the refractive index of the silica and the variation of the guided mode propagation constant as a function of wavelength; the PMD due to the random variation of the geometrical structure of the installed fibres creating the differential delay between the polarised optical fields of the linearly polarised weakly (LPWG) guided mode. This is the first-order PMD effect. Furthermore the first PMD effect is also wavelength-dependent thus there exists a chromatic PMD, the second order PMD effect. For low transmission line rate (<2.5 Gbps) the PMD effect is not noticeable. It is however very critical for 10 Gb/s and 40 Gb/s and beyond transmission rates. It is thus very important for optical system design to develop an accurate modelling platform taking into considerations of these PMD effects.

The usual technique for modelling an optical propagation was through implementing numerical solutions to the one-dimensional nonlinear Schrodinger equation (NLSE) based on the Fourier split-step method analysis [4]. However this formalism is no longer valid for modelling the optical transmission systems under significant effects of the PMD. This is due the polarisation of the guided modes forming the LP₀₁ (linearly polarised) mode of a single mode fibre. Therefore a new formalism is essential for developing the propagation of optical signals over the fibre. This would require a matrix formulation of the polarised modes. The use of Fourier Transform Split-Step methods are also not suitable for most network simulation problems and required high computational time. Therefore, it is necessary to base the simulation of the polarised lightwaves in the time-domain.

The principal objectives of this paper are thus: (i) To formulate the propagation equations for the polarised modes propagating over different types of single mode optical fibres, eg. Standard optical fibres with significant chromatic dispersion, dispersion shifted fibres and/or dispersion compensated and flattened fibres.(ii)To formulate the numerical solution to the propagation equation using a time domain approach based on the split method algorithms. (iii)To develop a design platform referred as **OcSim**; (iv) To incorporate several DWDM optical channels in the propagation equations and algorithm (vi) To incorporate other optical components such as optical transmitters, optical in-line amplifiers, optical in-line compensators etc into the modelling platform (vii) To demonstrate the OcSim simulator on MATLAB[®] for Windows operating environment.

This paper is thus organised as follows: **Section 2** concerns with the preliminary development of the propagation equations. This section investigates the theoretical foundation of fibre propagation and parameters required for the implementation of the OcSim package; **Section 3** is concerned with the formulation of the numerical solution to the propagation equations. This section provides the reader with the calculations and implementations of the design parameters; **Section 4** presents a case study of two different optical communication systems. The first example looks at the simulation of a 10 Gb/s DWDM

system and the second example looks at the simulation of a 40 Gb/s system, finally **Section 5** summarises the key findings of the paper.

2. The Propagation equation

2.1 Generic dispersion in single mode fibres

In optical fibres, dispersion is the consequence of the wavelength dependence ($dn/d\lambda$, where n is the refractive index and λ is the wavelength) between the optical fibre and optical signal, caused by interaction between the matter and light [5]. The main advantage of using single mode fibre is its ability to propagate energy in a single mode and thereby eliminate multimode distortion. However, the velocity of propagation of the optical signal in a single mode fibre is wavelength dependant due to chromatic dispersion. The variation of the group velocity of the optical signal, results in different frequency components travelling with slightly different group delays, thus arriving at the end-point at slightly different times. This phenomenon results in group-velocity dispersion (GVD), or intramodal dispersion. Chromatic dispersion consists of two contributions: (i) wavelength dependence of the optical signal on the refractive index of the fibre known as material dispersion; and (ii) a proportion of the light also travels in the cladding of the fibre, which has a different refractive index again and therefore propagates light through it at a different speed to the core, the waveguide dispersion.

When an optical signal is modulated and transmitted along a Single Mode Fibre, dispersion occurs, the propagation constant β with optical frequency [6] and can be described by the Taylor series around the centre carrier frequency as

$$\beta(\omega) = \beta(\omega_0) + \beta'(\omega - \omega_0) + \frac{1}{2}\beta''(\omega_0)(\omega - \omega_0)^2 + \frac{1}{6}\beta'''(\omega - \omega_0)^3 + \dots$$

Eq. 1

where ω_0 represents the nominal optical carrier frequency. The group delay τ_g can be related to the propagation constant by:

$$\tau_g = \frac{L}{V_g} = L \left\{ \frac{\partial \beta}{\partial \omega} \right\}$$

Eq. 2

Substituting (1) to (2), τ_g can be re-written as

$$\tau_g(\omega) = L \left[\beta'(\omega_0) + \beta''(\omega_0)\Omega + \frac{1}{2}\beta'''(\omega_0)\Omega^2 + \dots \right]$$

Eq. 3

Where Ω refers to the complex envelope $(\omega - \omega_0)$ and can be related to the wavelength variation Δ and

λ by:

$$\Omega = -\frac{2\pi c}{\lambda^2} \Delta\lambda$$

Eq. 4

By letting $\Delta\lambda$ be the spectral width of the source, the amount of pulse broadening can be estimated to [7]:

$$\Delta T = L \left(\frac{-2\pi c}{\lambda^2} \right) \beta''(\omega_0)$$

Eq. 5)

so that

$$D = -\left(\frac{2\pi c}{\lambda^2} \right) \beta_2$$

Eq. 6

where D is second order dispersion parameter defined as the variation of the travel time due to the wavelength dependence per unit length L. The D value near the 1550nm window is 17ps/(Km-nm). The chromatic dispersion of corning SMF-28 fibre operating near the 1550nm window can be fully

accounted for by the second order term of the propagation constant β as seen from Eq. 3. In our modelling platform OcSim the value of β_2 was calculated at the desired wavelength using Eq. 3. It is also possible to obtain fibres with the zero-dispersion point shifted to a value near 1550nm or any other desired value. These types of fibres are called dispersion-shifted fibres (DSF). Employing DSF does not completely eliminate chromatic dispersion as the wavelength dependence of D also causes pulse broadening. The dispersion slope can be written using Eq. 3 as

$$\frac{dD}{d\lambda} = \left(\frac{2\pi c}{\lambda^2}\right)^2 \beta_3 + \left(\frac{4\pi c}{\lambda^3}\right) \beta_2$$

Eq. 7

In OcSim the dispersion slope was evaluated by either using the difference approximation of the dispersion curve in MATLAB[®] or directly from the fibre specifications.

2.2 Polarization Mode Dispersion

PMD plays a vital role in high bit rate long haul communication systems employing dispersion-shifted fibres [9]. PMD is caused by the asymmetrical nature of practical optical strands. This asymmetry causes the light waves in one polarization axis to move faster or slower than the other principle axis. The separation of the two orthogonal pulses due to PMD is measured in terms of Differential Group Delay (DGD) $\Delta\tau$.

Although it is possible to develop propagation equation for the PMD effect, the simulator made use of the existing statistical model [9] for the inclusion of PMD effects. In this model the DGD value spreads over the fibre span ΔZ in the form of a Maxwellian distribution. The mean value of $\Delta\tau$ in the statistical model characterises the PMD of the fibre with the quantity δ_x measured in term $\text{ps}/\sqrt{\text{km}}$. In OcSim, the PMD over the span ΔZ was characterised by this value of δ_x which is typically around 0.1-0.5

ps/\sqrt{km} for installed fibres. The value of δ_x also depends on the frequency spread of the optical signal. Fibre loss is another mechanism that limits the performance of the fibre by reducing the average launched power. The power attenuation inside the fibre is governed by the equation by [7]:

$$\frac{\partial P}{\partial Z} = -\alpha P$$

Eq. 8

The scalar term α denotes the attenuation coefficient and P is the average optical power. In OcSim, attenuation coefficient α over the each window was assumed to be a constant.

Nonlinear effects in fibre have a significant impact in the performance of the DWDM optical fibre systems [11]. Nonlinearities can result in attenuation, loss and cross-channel interference. The effects of nonlinearity can place limitation to the bit rate and channel spacings of DWDM communications systems. OcSim takes into account the two most prevalent nonlinear effects that limit DWDM systems: self-phase modulation (SPM) and cross-phase modulation (XPM). SPM is caused by the variations in the power of an optical signal, resulting in the change in phase of the system and is given by:

$$\phi_{NL} = \gamma P_{in} L_{eff}$$

Eq. 9

where the parameter γ is the nonlinear coefficient of the fibre with an average optical input power P_{in} and an effective fibre length L_{eff} . XPM results from the shift in phase of an optical signal due to two or more simultaneous channels travelling inside a fibre. Therefore, XPM plays a vital role in the transmission of the DWDM signals. The phase shift of the j th channel is given by [4]

$$\phi_j^{NL} = \gamma L_{eff} [P_j + 2 \sum_{m \neq j}^M P_m]$$

where M is the total number of DWDM channels and P_j is the corresponding input power. In our modelling package OcSim, the value of γ was considered a constant along the length of the fibre having a typical value of $2 \text{ W}^{-1}\text{Km}^{-1}$.

2.3 Field Propagation Equation

The propagation equation of an optical pulse in its single mode is well established in the form of nonlinear Schrodinger equation (NSE) [7]. In order to include the two modes of propagation, the NSE should be re-written in a vector form. A useful derivation of the vector or bimodal propagation equation is given in [9] as:

$$\frac{\partial \underline{A}}{\partial z} + \left\{ \beta_1 \frac{\partial}{\partial t} - \frac{j}{2} \beta_2 \frac{\partial^2}{\partial t^2} - \frac{1}{6} \beta_3 \frac{\partial^3}{\partial t^3} \right\} \underline{A} + \alpha \underline{A} = -j \frac{\gamma}{3} \begin{Bmatrix} A_x (3|A_x|^2 + 2|A_y|^2) \\ A_y (3|A_y|^2 + 2|A_x|^2) \end{Bmatrix}$$

here $\underline{A} = \begin{Bmatrix} A_x(t, z) \\ A_y(t, z) \end{Bmatrix}$ is the field amplitude vector corresponding with that presented in the NLSE [4].

The third order series expansions of the matrix $\underline{\beta}$ represent the dispersion terms of the fibre. The $\underline{\beta}_1$ term accounts for the pure delay of pulse propagation and possibly the PMD first order effect in the fibre while $\underline{\beta}_2$ and $\underline{\beta}_3$ terms account for the chromatic dispersions in the fibre. α is the linear propagation loss coefficient of the fibre. The propagation equation includes most of the phenomena affecting DWDM optical communication systems. Four-Wave Mixing (FWM) is another nonlinear phenomena of importance in DWDM, an effect that is not included in the developed propagation equation [12(*)

3. Modelling Platform

In order to perform an accurate computer aided modelling of single mode fibre propagation, a numerical solution to Eq. 11 should be implemented into the design. OcSim uses the split-step method in a time domain environment to numerically solve Eq. 11. The split-step method divides the fibre length into small steps of ΔZ over which the dispersive and nonlinear effects are considered to be acting individually of each other. The propagation of an optical pulse from Z to $Z+\Delta Z$ is shown in Figure 1.

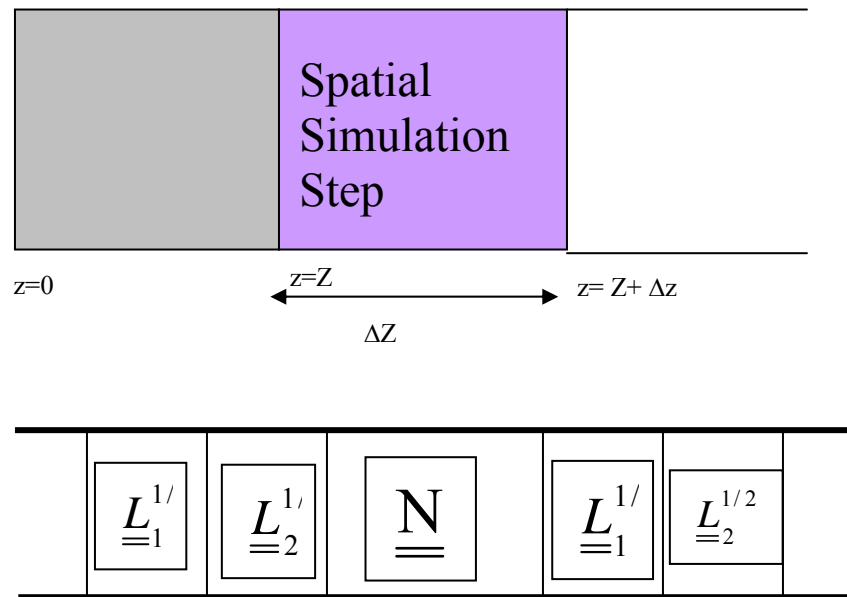


Figure 1 Schematic diagram of symmetrised split step model used for numerical simulations.

3.1 Time domain approach

The split step Fourier (SSF) procedure is normally used to examine the pulse propagation (SSF). The disadvantage of using FFT algorithms is that the pulse samples has to continuously converted between the frequency and time domain during the propagation steps. This approach for bi-modal propagation would result in high computational time. OcSim implements the spatial operators in the form of digital filters. The time domain approach allows for propagation in one domain. This would also allow for easy interactions with other optical devices such as transmitters and receivers making it ideal for optical networking in a DWDM system.

The pulse entering each spatial step would propagate into a purely dispersive medium represented by a digital filter $\underline{\underline{L}}_2^{1/2}$ for chromatic dispersion and then through a second digital filter $\underline{\underline{L}}_1^{1/2}$ representing PMD. The pulse then picks up the fibre nonlinearity and attenuation from the nonlinear operator $\underline{\underline{\tilde{N}}}(z')$ before propagating through the second purely dispersive segment. The transfer block representation of the spatial step is given in Figure 2. The subscript $1/2$ in the operators $\underline{\underline{L}}_1^{1/2}$ and $\underline{\underline{L}}_2^{1/2}$ describes the fact that both chromatic dispersion and PMD are present in the both halves of the split step.

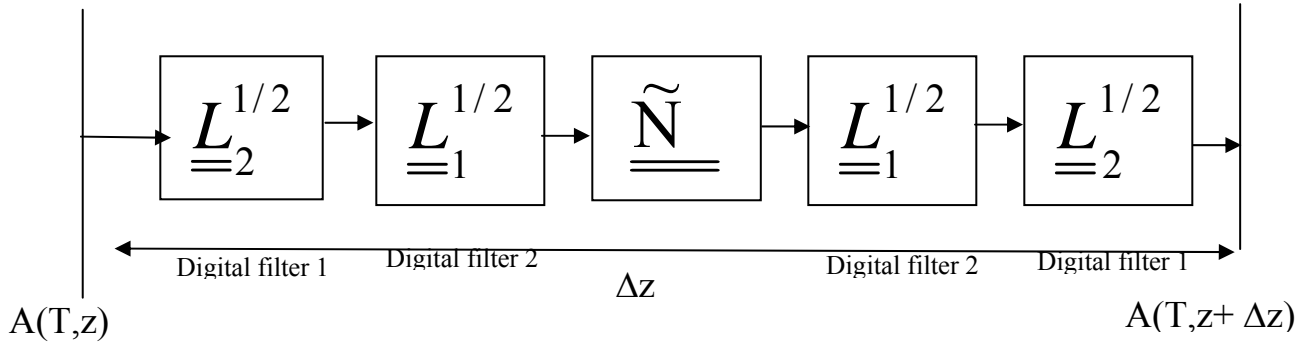


Figure 2 Cascade of optical transfer functions representing the vector field propagation.

The solution to Eq. 11 over each spatial step can be written in the following manner:

$$\underline{\underline{A}}(T, z + \Delta Z) \approx \underline{\underline{L}}_2^{1/2} \underline{\underline{L}}_1^{1/2} \exp\left(\int_z^{z+h} \underline{\underline{\tilde{N}}}(z') dz'\right) \underline{\underline{L}}_1^{1/2} \underline{\underline{L}}_2^{1/2} \underline{\underline{A}}(T, z)$$

Eq. 12

where the matrix operator $\underline{\underline{L}}_2^{1/2}$ is given by

$$\underline{\underline{L}}_1^{1/2} = \begin{bmatrix} H_d(z) & 0 \\ 0 & H_d(z) \end{bmatrix}$$

Eq. 13

where $H_d(z)$ represents the z-transform digital time domain filter that produces frequency dependant dispersion. In Eq. 12 it is assumed that chromatic dispersion distorts both modes of propagation equally. Meanwhile, PMD causes one of the principal axis to delay with respect to the other and therefore the matrix operator $\underline{\underline{L}}_1^{1/2}$ is given by:

$$\underline{\underline{L}}_1^{1/2} = \begin{bmatrix} H_p(z) & 0 \\ 0 & H_p(z) \end{bmatrix}$$

Eq. 14

Nonlinearity comprises of fibre nonlinearity and attenuation, and is included into design through the nonlinear operator $\underline{\underline{N}}(z')$ that depends only on distance z and therefore does not require time-domain filters for implementation. The nonlinear operator $\underline{\underline{N}}(z')$ can be directly obtained from the bi-modal propagation equation given in Eq. 11 and is given by:

$$\underline{\underline{N}}(z') = \begin{bmatrix} -j\frac{\gamma}{3}(3|A_x|^2 + 2|A_x|^2) - j\alpha & 0 \\ 0 & -j\frac{\gamma}{3}(3|A_y|^2 + 2|A_y|^2) - j\alpha \end{bmatrix}$$

Eq. 15

XPM can be included into the equation and for DWDM systems the matrix operator $\underline{\underline{N}}(z')$ becomes:

$$\begin{bmatrix} -j\frac{\gamma}{3} + \left(3|A_{jx}|^2 + 2|A_{jy}|^2\right) + 2 \sum_{m \neq j, m=1}^{m=N} \left(3|A_{mx}|^2 + 2|A_{my}|^2\right) - j\alpha & 0 \\ 0 & -j\frac{\gamma}{3} + \left(3|A_{jx}|^2 + 2|A_{jy}|^2\right) + 2 \sum_{m \neq j, m=1}^{m=N} \left(3|A_{mx}|^2 + 2|A_{my}|^2\right) - j\alpha \end{bmatrix}$$

Eq. 16

where the extra terms include the cross phase modulation (XPM) of the A_{jx} and A_{jy} modes of propagation with the N-1 adjacent channels A_{mx} and A_{my} respectively.

3.2 IIR filter for chromatic dispersion

As previously noted in Section 2, the chromatic dispersion is caused by the frequency dependence of the group delay associated with the optical wave. Chromatic dispersion results in distortion of the optical signal without directly affecting the amplitude of the signal. This allows the operator $\underline{\underline{L}}_2^{1/2}$ to be implemented as an all-pass filter with the group delay characteristics given as:

$$\tau_g(\omega) = L \left[\beta''(\omega_0)\Omega + \frac{1}{2}\beta'''(\omega_0)\Omega^2 \right]$$

Eq. 17

where the first term refers to the linear delay and the second term refers to the parabolic delay. The term all-pass refers to the fact that the filter has unit amplitude within the Nyquist bandwidth. If the Nyquist bandwidth is f_b then the sampling frequency f_s should be twice the optical bandwidth f_b . Therefore, the filter operates between the frequency domain given by $-\frac{1}{(2T_c)} \leq f \leq \frac{1}{(2T_c)}$ where T_c is the sampling time given by $1/f_s$

In OcSim an Infinite-impulse-response (IIR) time domain numerical filter was elected for representing the operator $\underline{\underline{L}}_2^{1/2}$. The IIR filters allowed for easy implementation of the all-pass filter compared with than most other types of discrete filters [14].

4. Design of IIR filters

The linear group delay is given as $(\Delta z / 2) \beta''(\omega_0)\Omega$ where L is substituted with the first half of the spatial step shown in Figure 2. This delay has to be represented with an all-pass filter capable of producing group-delay characteristics that change linearly with the frequency Ω . Although it is possible

to design such a filter from scratch, filters that produce fine approximations to linear delays are well developed [9][13] and one such approximation is given by [9]:

$$H_{lin}(z) = uv \frac{z - j\frac{1}{u}}{z - ju} \frac{z - \frac{1}{v}}{z - v}$$

Eq. 18

where u and v are real numbers. The matching of the pole-zero pair in Eq. 18 is characteristic to all pass filters with phase distortion [14]. The unit amplitude of the filter allows us to relate the two real numbers u and v by:

$$1 = 4 \frac{u^2(1-u^2)(1-v)^3}{v(1+u^2)^3(1+v)}$$

Eq. 19

The resulting group delay of the filter is thus given by:

$$\tau_{H_{lin}} = \tau_0 + 2T_c^2 \frac{u(1-u^2)}{(1+u^2)^2} \Omega$$

Eq. 20

The term τ_0 is a constant pure delay common to most digital filters and has no importance to chromatic dispersion. In OcSim, this pure delay was eliminated from the final design by shifting the pulse samples by a negative delay constant. The second term of Eq. 20 contains the desired linear group delay

response. The plot of the delay term $\frac{u(1-u^2)}{(1+u^2)^2}$ as a function of u shown in Figure 3 suggests that the

maximum value u can take is limited to ± 0.4 .

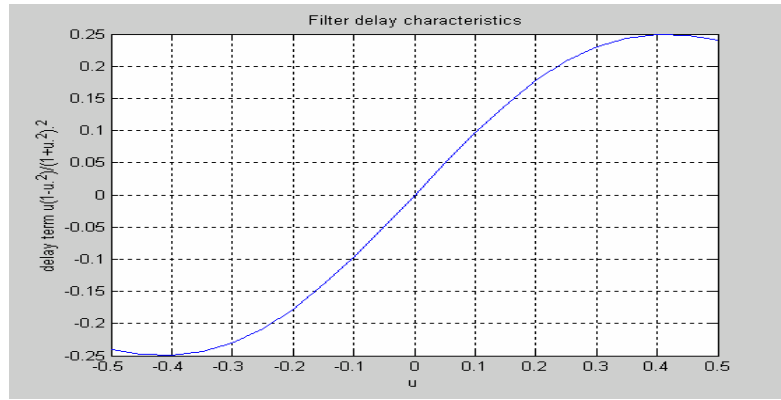


Figure 3 The plot of delay term $\frac{u(1-u^2)}{(1+u^2)^2}$ as a function of u.

Therefore, the total linear delay that can be obtained from a single filter is limited to around $\pm 0.5T_c^2\Omega$.

The required group delay of $(\Delta z/2)\beta''(\omega_0)\Omega$ for DWDM systems is certainly greater than the maximum delay that can be obtained from a single IIR filter. Cascading more filters solves the need for greater delay values [14]. The cascade arrangement shown in Figure 4 is simply obtained by passing the output from one filter to the next filter, which results in the group delay being added together.

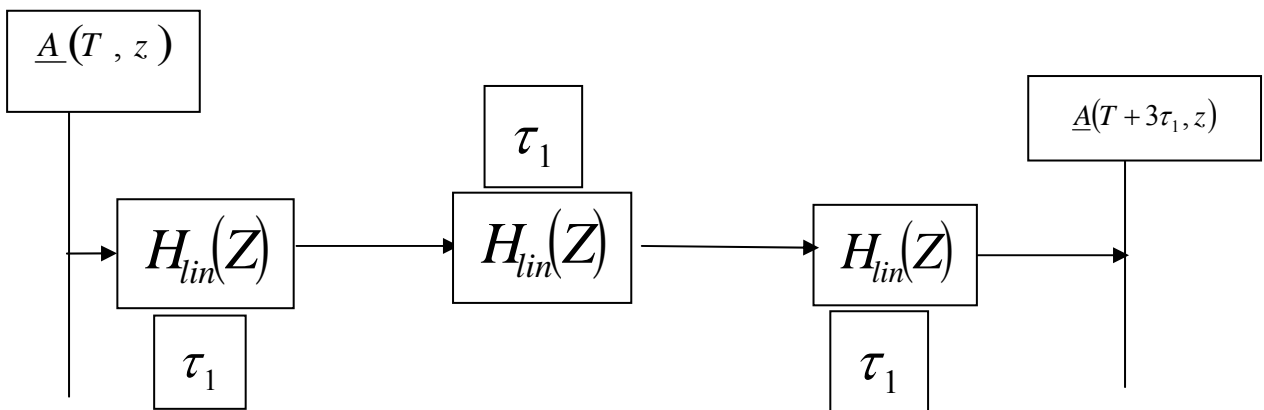


Figure 4 Cascade for obtaining greater group delay PMD effects.

The value of u was carefully chosen to minimise the error between the desired response and the obtained response. It was seen that operating at the maximum value of $\pm 0.5T_c^2\Omega$ led to fairly inaccurate results.

The optimal value for u , through trial and error, was found to be around ± 0.282 , which delivered a maximum delay of $\pm 0.4455 T_c^2 \Omega$ - a few percent below the theoretical maximum. Once the value of u is known, the value of v can be calculated directly from Eq. 19.

3.2.2 Performance of IIR filter

The performance of the IIR filter was carried out through an actual design procedure. It was decided that the testing was carried out using a single IIR filter avoiding the need for cascading. The design parameters are given in the Table 1 as:

Fibre characteristics	
Dispersion D	17ps/nm-Km
β_2	-21.632ps ² /Km
Operating Frequency f_0	1550nm
Sampling Time T_c	1.76 ps
ΔZ	$\approx 130m$

Table 1: The filter parameters for measuring filter performance

u parameter	-0.282
V parameter	0.13355

The value of T_c and ΔZ was carefully chosen to match the required delay $(\Delta z/2) \beta''(\omega_0) \Omega$ with the delay $2T_c^2 \frac{u(1-u^2)}{(1+u^2)} \Omega$ delivered by the filter with u set at the optimal value of -0.282 . The value In order to implement a Z-transform filter in MATLAB[®], the general form of the transfer function $H_{in}(z)$ is given by:

$$H(z) = \frac{B(z)}{A(z)} = \frac{b(1) + b(2)z^{-1} + \dots + b(nb+1)z^{-nb}}{a(1) + a(2)z^{-1} + \dots + a(na+1)z^{-nb}}$$

where $b(n)$ and $a(n)$ are the numerator and the denominator coefficients of the IIR filter with n a positive integer. Therefore (21) should be re-written in the form:

$$H_{lin}(z) = \frac{uv - (u + vj)z^{-1} + jz^{-2}}{1 - (v + ju)z^{-1} + juvz^{-1}}$$

where $b = [uv, -(u+vj), j]$ and $a = [1, -(v+ju), juv]$ are the vectors coefficients of the IIR filter. The group delay characteristic of the filter was plotted in MATLAB[®] using the “**grpdelay**” command. The plot of the linear group delay against the ideal group delay is shown in Figure 5.

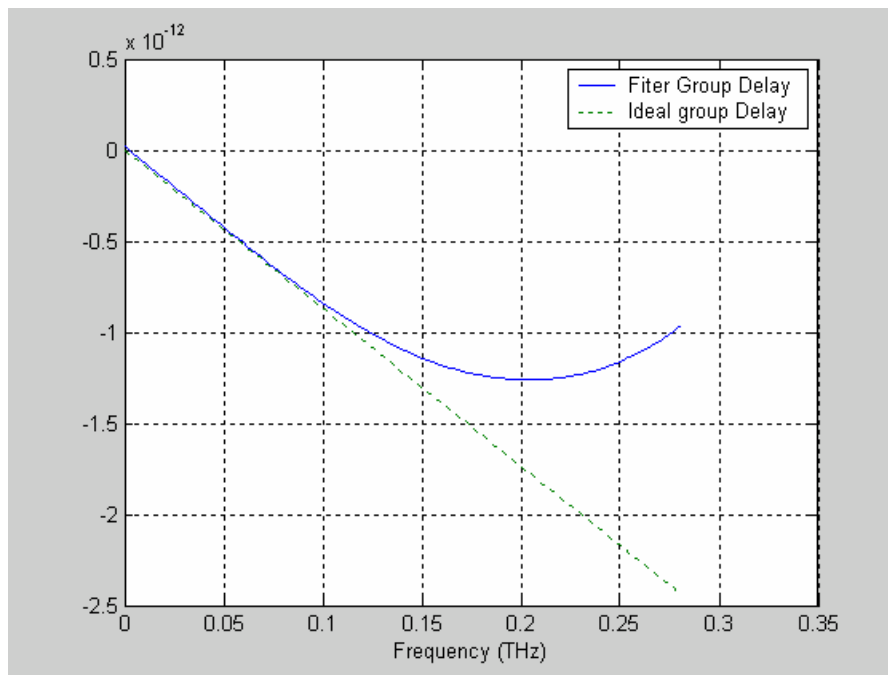


Figure 5 Comparison of the ideal group delay versus the IIR filter produced group delay

There is a good agreement between the desired group delay and the filter group delay for most part of the Nyquist bandwidth. Accuracy can be improved further by raising the power of the transfer function.

However, filter described in Eq. 22 allows for fairly accurate modelling of the frequency dependant dispersion and is used in OcSim for producing chromatic dispersion.

A similar procedure allows for the implementation of the higher order dispersion included by the β_3 term. The filter transfer function for the parabolic delay $\frac{\beta_3}{2} \Omega^2 \frac{\Delta z}{2}$ is given by [9]:

$$H_{par}(z) = v \frac{z - \frac{1}{v}}{z - v}$$

Eq. 23

where v is a real number characterising the filter with the group delay given by:

$$\tau_{H_{par}} = \tau_0 - T_c^3 \frac{v(1+v)}{(1-v)^3} \Omega^2$$

Eq. 24

Where the term τ_0 again represents the pure delay of the filter and the plot of $\frac{v(1+v)}{(1-v)^3}$ as a function of v defines a maximum allowable delay of the filter to $(T_c^3 / 8) \Omega^2$.

The chromatic dispersion filter $H_d(z)$ can now be represented as the combination of the linear and parabolic filters and is given by:

$$H_d(z) = H_{lin}(z) H_{par}(z)$$

Eq. 25

4.1 Inclusion of PMD phenomena

The PMD effect is included through the operator $\underline{L}_1^{1/2}$ and is treated statistically as mentioned in section 2.2. The simplest approach to include PMD is to delay one of the polarisation axis by $\Delta\tau$ relative to the other over each spatial step. The amount of delay $\Delta\tau$ is found directly from the fibre parameter δ_τ measured in term ps/ \sqrt{km} . An all-pass filter capable of producing such as pure delay is given by [14]:

$$H_p(z) = z^{-k}$$

Eq. 26

where k is a real number representing the amount of time samples. The total delay produced by the filter is given by:

$$\tau_p = k * T_c$$

Eq. 27

where T_c is the sampling time of the input signal. The transfer function z^{-1} indicates its delay characteristics against frequency. The problem of using such an approach is that only delays in multiples of T_c can be implemented. The PMD induced delay produced over a single step Δz is usually in the sub values of T_c . Filters producing sub- T_c values are much more complex than the filters given by Eq. 23. This problem was overcome by allowing the optical pulse to propagate over few spatial steps until the total delay is close to the delay produced with a single filter. This unit delay was applied to the appropriate axis and propagation was allowed to continue until the next unit delay was required.

4.2 Algorithm for the split step model

The split step method was incorporated into OcSim using the MATLAB[®] platform. A systematic approach was taken to implement the split step method in MATLAB[®] allowing for easy upgrade and maintainability.

As pointed out in section 3, the split step model can be expressed according to Eq. 12 and therefore various stages of the implementation of the propagation dynamics details are given as follows:

- Stage 1: This refers to the first half chromatic dispersion only region. In this region, both PMD and nonlinearity are absent. Therefore the amplitude of the resulting dispersed pulse can be expressed as:

$$\underline{A}_d\left(T, z + \frac{\Delta z}{2}\right) \approx \underline{L}_2^{1/2} \underline{A}(T, 0)$$

Eq. 28

Where $\underline{A}(T, 0)$ describes the pulse at the start of propagation. The dispersion operator $\underline{L}_2^{1/2}$ can be replaced with Eq.3.1.2 to give:

$$\underline{A}_{d1}\left(T, z + \frac{\Delta z}{2}\right) \approx \begin{bmatrix} H_a(z) & 0 \\ 0 & H_a(z) \end{bmatrix} \underline{A}(Z, z)$$

Eq. 29

OcSim implemented Eq. 23 using the MATLAB[®] command “**filter**”. The filter function filters a data sequence using a digital filter, which works for both real and complex inputs. The MATLAB[®] syntax for the filter function is given by:

$$y = \text{filter}(b,a,X)$$

where X is a vector representing the data or time samples to be filtered with the filter $H_d(z)$ described by numerator coefficient vector b and denominator coefficient vector a .

- Stage 2: The first segment also corresponds to the step where the pulse propagates through a stage with only PMD effect taking place. The resulting amplitude \underline{A}_{p1+d1} with $\underline{L}_1^{1/2}$ replaced with (31) is given by:

$$\underline{A}_{p1+d1}\left(T, z + \frac{\Delta z}{2}\right) \approx \begin{bmatrix} H_p(z) & 0 \\ 0 & 1 \end{bmatrix} \underline{A}_{d1}\left(T, z + \frac{\Delta z}{2}\right)$$

where the filter $H_p(z)$ in Eq. 31 producing the differential delay, was yet again implemented in OcSim using the MATLAB[®] “filter function”. The pulse in the x-direction is delayed and the pulse in the y-direction propagates without any delay. The direction to which the delay is applied is arbitrary, but it is crucial that the amount of delay is applied to only one of the propagating modes.

- Stage 3: In this stage, only nonlinear delay is present and the output from stage 1 is propagated through the lumped nonlinear region according to the expression:

$$\underline{A}_N\left(T, z + \frac{\Delta z}{2}\right) \approx \exp\left(\int_z^{z+h} \underline{\tilde{N}}(z') dz'\right) \underline{A}_{p1+d1}(T, z)$$

Where the integration can be performed by employing the trapezoidal rule and is approximated integral is given by:

$$\int_z^{z+h} \underline{\underline{\tilde{N}}}(z') dz' \approx \frac{h}{2} \{ \underline{\underline{\tilde{N}}}(z) + \underline{\underline{\tilde{N}}}(z + \Delta z) \}$$

Eq. 33

The implementation of Eq. 33 is complicated by the need to identify $\underline{\underline{\tilde{N}}}(z + \Delta z)$ at the mid-point of the split step. Therefore an iterative procedure given in [15] is followed with the initial expression of $\underline{\underline{\tilde{N}}}(z + \Delta z)$ set to $\underline{\underline{\tilde{N}}}(z)$. This value of $\underline{\underline{\tilde{N}}}(z + \Delta z)$ is substituted back into Eq. 12, which in turn is used as the initial step to calculate the new propagation of $\underline{\underline{\tilde{N}}}(z + \Delta z)$ from Eq. 1. The steps for evaluating $\underline{\underline{\tilde{N}}}(z + \Delta z)$ are the following steps:

$$\text{Step 1: } \underline{\underline{A}}_{d1} \left(T, z + \frac{\Delta z}{2} \right) = \underline{\underline{L}}_2^{1/2} \underline{\underline{A}} (T, z)$$

$$\text{Step 2: } \underline{\underline{A}}_{p1+d1} \left(T, z + \frac{\Delta z}{2} \right) = \underline{\underline{L}}_1^{1/2} \underline{\underline{A}}_{d1} \left(T, z + \frac{\Delta z}{2} \right)$$

$$\text{Step 3 : } \underline{\underline{A}}_{N1} \left(T, z + \frac{\Delta z}{2} \right) = \exp \left(\frac{h}{2} \{ \underline{\underline{\tilde{N}}}(z) + \underline{\underline{\tilde{N}}}(z + \Delta z) \} \right) \underline{\underline{A}}_{p1+d1} \left(T, z + \frac{\Delta z}{2} \right)$$

$$\text{Step 4: } \underline{\underline{A}}_{p1+N1} \left(T, z + \frac{\Delta z}{2} \right) = \underline{\underline{L}}_1^{1/2} \underline{\underline{A}}_{p1} \left(T, z + \frac{\Delta z}{2} \right)$$

$$\text{Step 5: } \underline{\underline{A}}_{p1+d1+N1} \left(T, z + \frac{\Delta z}{2} \right) = \underline{\underline{L}}_2^{1/2} \underline{\underline{A}}_{p1+N1} \left(T, z + \frac{\Delta z}{2} \right)$$

Hence, the predicted $\underline{\underline{\tilde{N}}}(z + \Delta z)$ can be given by:

$$\underline{\underline{\tilde{N}}}(z + \Delta z) = -j\gamma \left\{ \left| \underline{\underline{A}}_{d1+p1+N1} \left(z + \frac{\Delta z}{2}, T \right) \right|^2 \right\} - \alpha$$

Eq. 34

where the operator $\underline{\underline{\tilde{N}}}(z + \Delta z)$ for DWDM system contains the SPM and XPM terms described by Eq.

34. This value of $\underline{\underline{\tilde{N}}}(z + \Delta z)$ is substituted back into step 1 for a better approximation of $\underline{\underline{\tilde{N}}}(z + \Delta z)$.

Once the nonlinear operator $\underline{\underline{\tilde{N}}}(z + \Delta z)$ is known, the pulse can be transmitted over the non-linear region

by using:

$$\underline{\underline{A}}_N \left(T, z + \frac{\Delta z}{2} \right) = \exp \left(\frac{h}{2} \{ \underline{\underline{\tilde{N}}}(z) + \underline{\underline{\tilde{N}}}(z + \Delta z) \} \right) \underline{\underline{A}}_{p1+d1} \left(T, z + \frac{\Delta z}{2} \right)$$

Eq. 35

- Stage 4: This corresponds to the second segment of the split step. The pulse is passed over a region containing only PMD. The resulting expression is given by:

$$\underline{\underline{A}}_{p1} \left(T, z + \Delta z \right) \approx \begin{bmatrix} H_p(z) & 0 \\ 0 & 1 \end{bmatrix} \underline{\underline{A}}_{-N} \left(T, z + \Delta z \right)$$

Eq. 36

where the differential delay is again applied to one of the principle axis.

Stage 5: Finally the pulse is propagated over a purely dispersive region described by:

$$\underline{\underline{A}}_{d1+p1} \left(T, z + \frac{\Delta z}{2} \right) \approx \begin{bmatrix} H_d(z) & 0 \\ 0 & H_d(z) \end{bmatrix} \underline{\underline{A}}_{-} \left(T, z + \Delta z \right) \quad (37)$$

Stage 6: For further propagation can be implemented using the output optical field amplitude as the input to the next stage and repeat stages 1-6.

4.3 Representation of the optical signal

In order to propagate the optical pulse, a method to represent the optical signals must be first developed. The type of line coding, formulation of the optical signal and the sampling rate are some of the issues needs consideration. Most of the design issues regarding the optical source representation are well developed in our previous report [15] .

In OcSim, the challenge was to represent the optical signal in a bi-modal state thus allowing for both modes of propagation. The most common schemes available are, non-return to zero (NRZ), return to zero (RZ) and Manchester (MAN). Our modelling presented is for NRZ format, as they have small bandwidth requirements and high channel capacity.

4.4 Optical source modelling

NRZ signal is considered with modulating current pulse shape in the form

$$I_p(t) = \begin{cases} I_{\max} (1 - \exp(-t / t_{rise})^2), & \text{bit1} \\ I_{\max} \exp(-t / t_{rise})^2, & \text{bit0} \end{cases}$$

Eq. 37

The modulation current is given by

$$I_m(t) = I_{bias} + I_p(t) \exp(j\omega_m t)$$

Eq. 38

where ω_m is the modulation frequency. The resultant optical field of the modulated signal is computed for transmission in the fibre:

$$E_R(t) = \sqrt{P_S(t)} \exp(j(\omega_c t + \phi))$$

Eq. 39

The resulting electric field can be linked with its components by using the relationship:

$$E_R^2(t) = E_x^2 + E_y^2$$

Eq. 40

where $E_R^2(t)$ represents the normalised power launched into the fibre and is measured in watts.

In OcSim, the resultant field at the start of the tem $E_R^2(0,t)$ can be easily calculated and by assuming

$E_x = E_y$ at the initial step we obtain:

$$E_x(0,t) = E_y(0,t) = \frac{E_R(0,t)}{\sqrt{2}}$$

Eq. 41

The propagation modes $E_x(0,t)$ and $E_y(0,t)$ can now be substituted into the amplitude vector $\underline{A}(T,0)$ and transmitted using the theory developed in previous sections.

4.5 Sampling of the input waveform:

The number of sampling points N required for optical signals with a time window T_w and sampling frequency f_s is by the equation:

$$N = \frac{T_w}{T_c} = T_c \times f_s$$

Eq. 42

where the sampling points N is rounded of to the nearest power of 2 and the Sampling time $T_c = 1/f_s$ follows the Nyquist rate, which states that for a continuous signal to properly recovered, the sampling rate should be higher than or equal to twice the highest frequency contained in the signal. Therefore, signal with carrier frequency f_c results in the sampling frequency of $2f_c$. The carrier frequencies of optical signals are in the order of THz resulting in large values of f_s which in turn results in large values of N . Previously we eliminated this problem by defining an offset frequency f_{off} that would shift the optical carrier frequencies to a lower value and thus lowering the value of f_s .

In OcSim it is critical that the number of sampling points is reduced to minimum as the optical signal in OcSim is contained in a bi-modal vectorial form. The other parameter that affects the sampling points of the signal is time window parameter T_w . In general, a low bit-rate signal would occupy a larger window than the high-bit rate window. For example, the total time required to represent a 8-bit window 10 Gb/s signal is lot greater than the time required to represent a 8-bit window 40 Gb/s signal.

In this simulator, the amount of PMD delay for each spatial step is obtained through fibre parameter δ_r and then accordingly applied to each spatial step. A better solution would be randomly generate the amount of differential delay at each spatial step in accordance to the Maxwellian distribution and then apply this delay to the polarisation modes.

5. Case study

In order to illustrate the performance of the simulator, two different examples were considered. The first example looks at the performance of the commonly deployed 10 Gb/s optical communication systems. In order to address the effects of PMD on optical communication systems, a second simulation at 40Gb/s was also performed. It was also decided to perform the simulations with the commercially available optical fibres

5.1 Simulation of 10Gpbs System

The popular **Corning SMF-28™** single mode fibre was used to simulate the 10Gb/s system. The fibre specifications of Corning SMF-28™ are given in Table 2:

Fibre Specifications	
Operating Wavelength (nm)	1550
Dispersion @ 1550nm (ps/nm-Km)	17
Attenuation@ 1550nm (DB/Km)	0.2
Dispersion slope (ps/nm ² .Km)	0.086
Nonlinear parameter (W ⁻¹ Km ⁻¹)	2
Average PMD (ps/√Km)	0.1

Table 2 Corning SMF-28™ fibre specifications

Due to the increasing popularity of incorporating DWDM into 10Gb/s systems, the simulation was carried out with four-channel link spaced according to the DWDM grid spacing. The number of channels could easily be increased further but was kept down to four for maintaining a reasonable CPU time. The simulation setup is tabulated in Table 3.

Simulation Setup	
Bit Rate (Gbps)	10
Usable BandWidth (GHz)	700
Laser type	DFB
Laser Linewidth (GHz)	30
Simulation Timestep (ps)	0.73
Simulation Distance (Km)	50
Simulation Step (m)	500

Table 3 Simulation set up for propagation of 10Gb/s

The simulation was triggered with an 8-bit sequence at 10Gb/s. The optical power of one of the channels is given Figure 7. The same sequence was chosen for rest of the channels for simplicity.

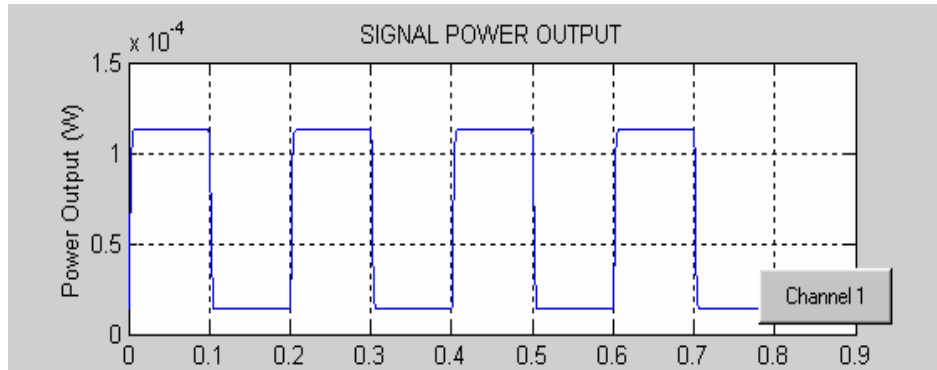
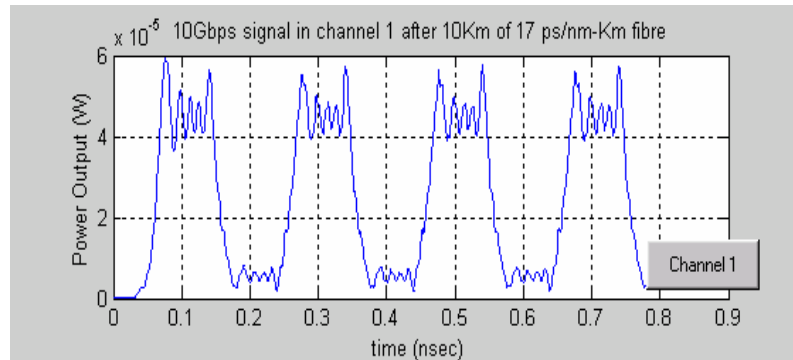


Figure 6 Signal power channel output at the start of transmission

The power spectral density for the multiplexed channels with a frequency offset of 193.0 THZ is given in Figure 8. The bandwidths were chosen as to allow for the central frequency of the simulation band to be situated at 1550nm. The operating frequencies of the channels are at 1550.067nm, 1550.868nm, and 1548.267nm and 1548.467nm respectively in accordance to the ITU grid spacing.

The output power of the channels and its power density plots are given in Figure 7 the channels at distance of 10Km of propagation with all the relevant fibre effects are shown is in given in Figure 7.



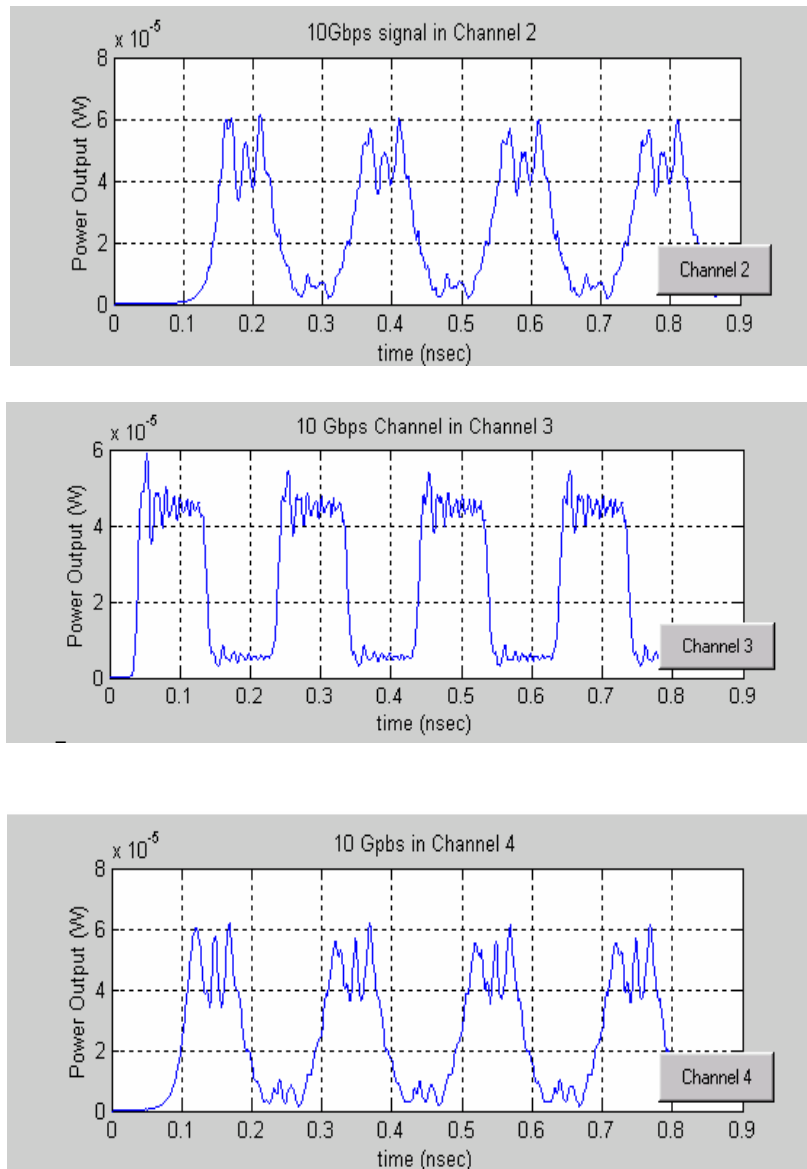


Figure 7 The 10 Gbps transmitted bits after 10 Km of propagation

The resulting power spectrum after 10 km of simulation is given in Figure 8 below.

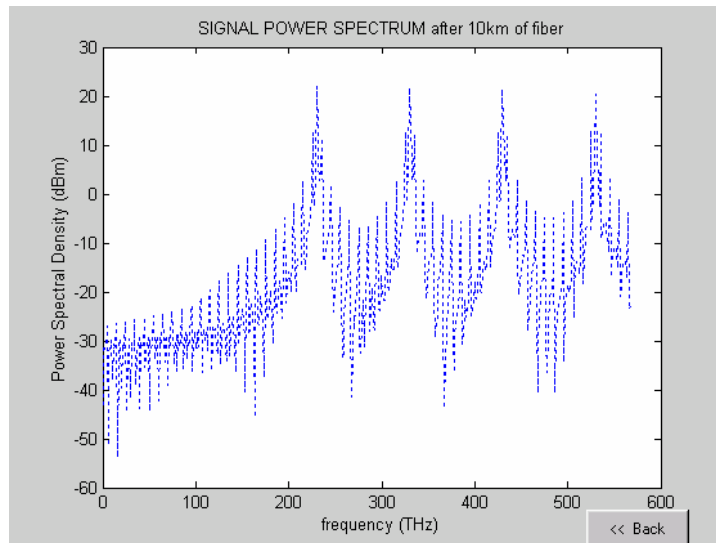
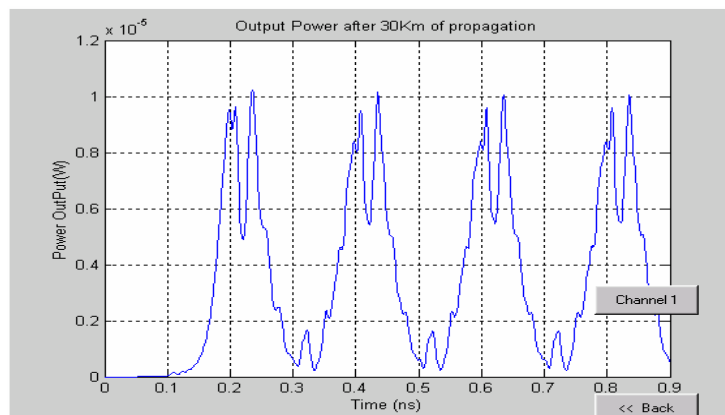


Figure 8 Resulting output spectrum of multiplexed channels after 10 Km of the 10 Gb/s channel

The comparison of the resulting pulse with the original pulse shown in Figure 6 shows the limitations of the optical communication systems. The drop in the output power is the result of the attenuation loss associated with the fibre. Chromatic dispersion, PMD and the fibre nonlinearity accounts for the distortion of the signal. The differences in the dispersion characteristics is seemingly due to the differences in the propagation constant β of the multiplexed signals which was assumed to be the same as the value of β at 1550nm. The fibre effect with distance was investigated by propagating the signal to 30Km. The obtained results are shown in Figure 9.



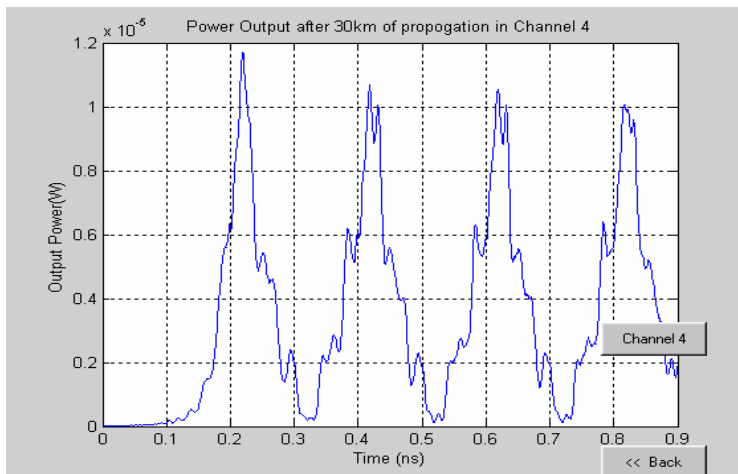
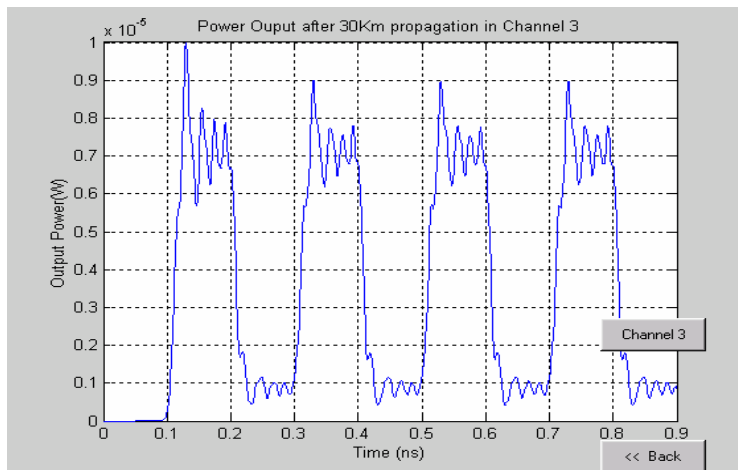
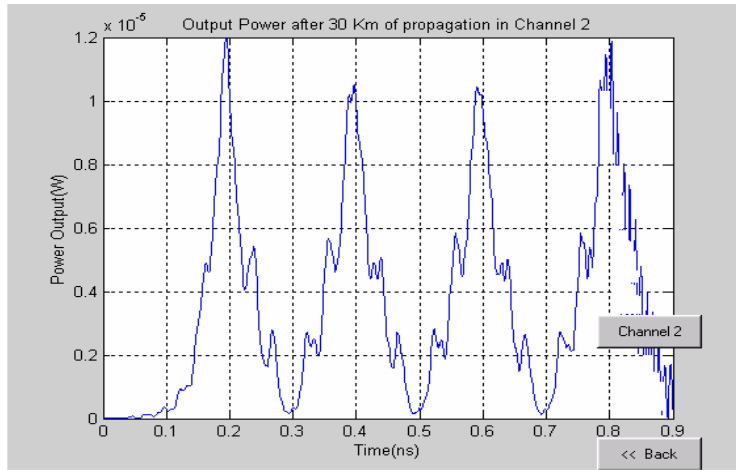


Figure 9 The power output channels 1 to 4 after 30 km of propagation

The wave output at 30Km shows a number of differences with the 10 km output shown in Figure 7 and Figure 8. The power loss increases linearly with distance. The dispersion and distortion of the signals

are further increased with distance of propagation. Propagating the signals in a fibre with negative dispersion or placing a compensating filter after every few kilometres are the usual methods of compensating for dispersion effects in fibre communication systems. The propagation distance for a 10 Gb/s system is usually limited to 50Km after which amplifiers and compensators are required for further propagation.

5.2 Simulation of a 40 Gb/s communication system

These increasing demand of optical communication systems have brought about the need for channels capable of propagating 40 Gb/s signals. The decrease in optical pulse width causes even severe limitations to the amount of pulse broadening. The effects such as PMD therefore play a vital role in the performance of the high bit rate channels.

The 6910 TeraLight™ fibre from ALCATEL was chosen for the propagation of the 40 Gb/s signals. The low chromatic dispersion of these fibres allows for the PMD effect to play a major part in the pulse broadening. The 6910 TeraLight™ specifications are given in Table 4.

Fibre Specifications	
Operating Wavelength (nm)	1550
Dispersion @ 1550nm (ps/nm-Km)	8
Attenuation@ 1550nm (DB/Km)	< 0.25
Dispersion slope (ps/nm ² .Km)	0.058
Nonlinear parameter (W ⁻¹ Km ⁻¹)	2
Average PMD (ps/√Km)	0.1

Table 4 TeraLight™ 6910 fibre specifications

The simulation set up was similar to the 10 Gb/s system but the number of channels was limited to one for simplicity. Although the PMD value of the fibre was given to be 0.1ps/√Km, the value is increased to 0.5 ps/√Km in order for visualising the distortion effects. The bit sequence at the start of simulation is given in Figure 10.

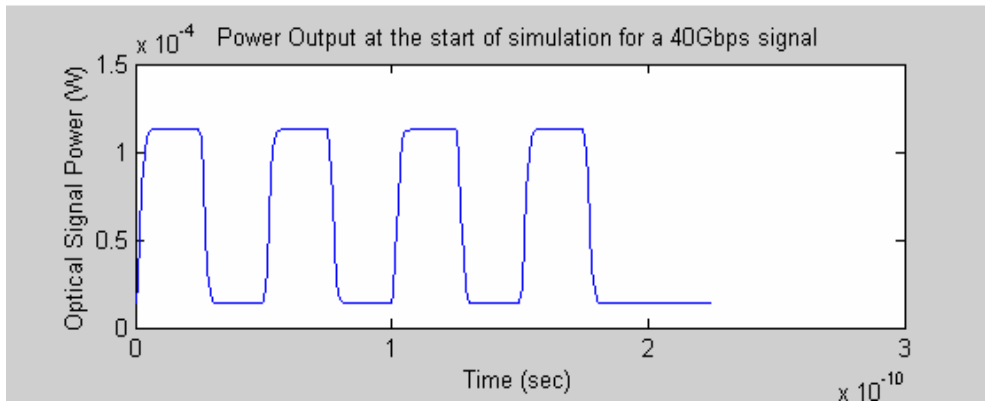


Figure 10 Output power of channel 1 at the start of simulation for a 40G/s system

The signal was allowed to propagate for 30 km and the total the resulting waveform is shown in Figure 11.

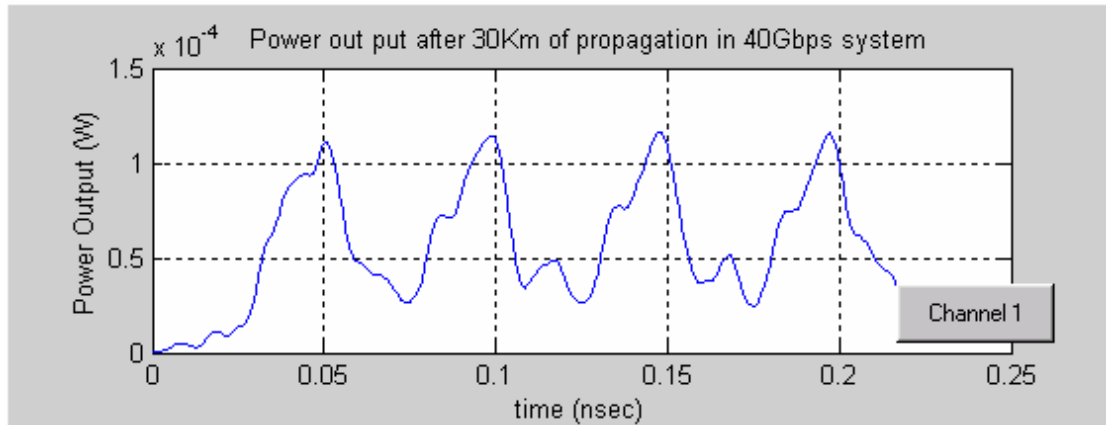


Figure 11 Output signal power of channel 1 after 30 kms of propagation

In order to measure the amount of PMD induced dispersion in Figure 11, the optical pulse was allowed to propagate with only PMD effect taking place over the length of the fibre. The result of one such propagation is shown in Figure 12 where the fibre is propagated through distances of 30 and 70 km with only PMD taking place. The pulse broadening becomes can be seen at around 30 km and becomes an issue at around 70 km. It is clear from Figure 12 that PMD has plays a vital role in the transmission of high bit-rate, long-haul optical communication systems.

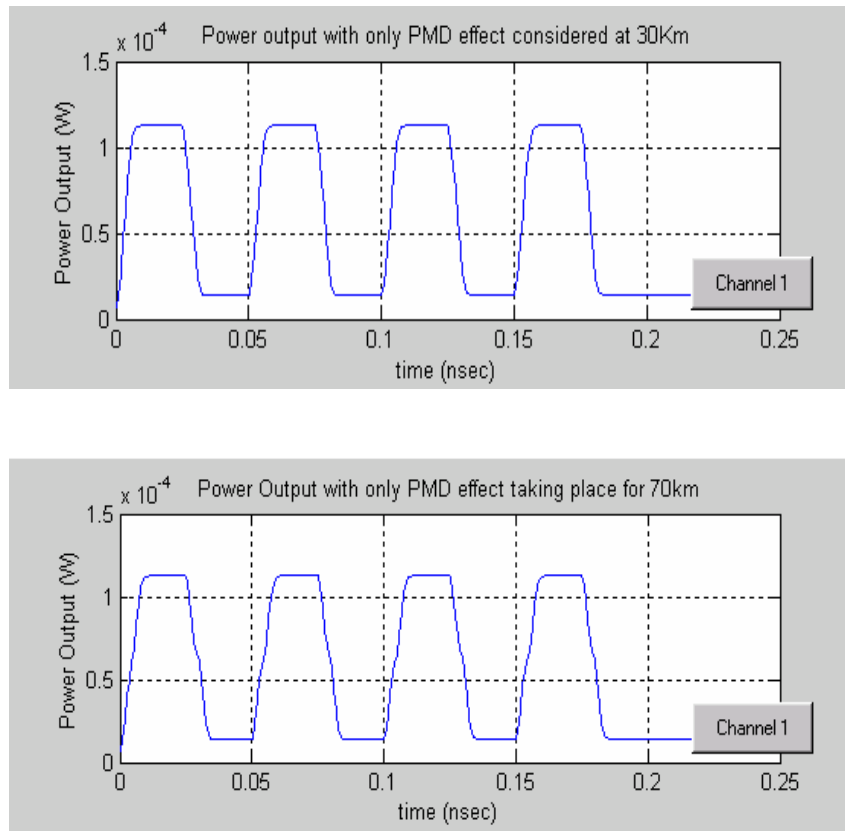


Figure 12: Effects of PMD on channel 1 and channel 2 after transmission

6. Conclusions

This paper presents a modelling platform for the propagation of several multiplexed signals, taking into account all the relevant nonlinear and polarisation related effects. For modelling of PMD related effects, a vector propagation equation describing the two modes of propagation should be established. The development of the bi-modal equation should follow closely with the well-developed Nonlinear Schrodinger Equation. The need to transmit both modes of propagation places heavy burden on the computational time. The best approach to cut down on CPU time is to perform the simulation in a time domain environment. This allowed implementing the Split Step Method in entirely a single domain.

The chromatic dispersion was best implemented using an IIR-discrete filter, which was capable of producing the required delay characteristics. A statistical approach can be used to find the amount of differential delay produced by PMD on each split step. This delay can be designed as a filter and added to any one of the propagation modes for producing the required delay.

The performance of the DWDM systems was demonstrated using the simulation package. The simulation platform allows for possible inclusion of effects such as FWM, which are also important for DWDM systems. Other devices such as PMD compensators can be easily included into the MOCSS (Monash optical Communication System Simulator) simulation package.

7. References

- [1] www.NortalNetworks.com , Products and services.
- [2] www.onet.on.ca,
- [3] P.S.Henry, S. D.Personic, Coherent Lightwave Communications, NewYork, IEEE press, 1990
- [4] Agrawal, G.P, Nonlinear Fibre optics. New York: Academic, 1995.
- [5] P. Rajappa, Introduction to light wave communication systems: Boston 1997
- [6] G.Cancelliri, Single-Mode Optical Fibres, Pergamon press
- [7] G. P.Agrawal, Fiber Optic communication systems: J. Wiley, 1992.
- [8] www.iec.org/online/tutorials
- [9] Andrea Carena, V. Curri, R. Gaudino, P. Poggiolini, and S. Benedetto., “A Time-Domain Optical Transmission System Simulation Package Accounting for Nonlinear and Polarisation-Related Effects in fiber”, IEEE J. Selected Areas Comms., vol. 15, no 4 , May 1997.
- [10] www.corningfiber.com
- [11] S.V. Kartalopoulos, Introduction to DWDM technology: data in a rainbow:
New York Press
- [12] B. Mukherjee, Optical communication networks: New York.
- [13] “www.Stanford.edu”
- [14] J.Prokais, Advanced Digital Signal Processing: New York, Macmillan Pub.
- [15] L.N. Binh”*Ultra-long haul Ultra-high speed optical communications systems*”, Monash university 1999.